Table 2 Comparison of aerodynamic characteristics between the solutions with different rate coefficients; ellipses of 10% thickness, at the altitude of 50 km and angle of attack of 20 deg

	$\gamma = 1.4$	Standard rates	Rates × 10
C_L	0.3206	0.3175	0.3090
C_D	0.1531	0.1515	0.1478
CP Shift, %	0	−0.14	−0.081

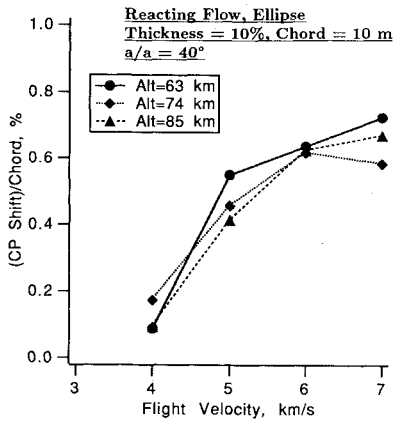

Fig. 4 CP Shift due to real-gas effects for the ellipse of 10% thickness as a function of V, for the chord length of 10 m, $a/a = 40$ deg, and for the altitudes of 63, 74, and 85 km.

of 0.6 ± 0.2% has been observed at angles of attack between 20–40 deg.[4] The CP shifts calculated in the present work are also of the same order.

References

[1]Park, C., and Yoon, S., "Calculation of Real-Gas Effects on Airfoil Aerodynamic Characteristics," AIAA Paper 90-1712, June 1990.

[2]Park, C., and Yoon, S., "Calculation of Real-Gas Effects on Blunt-Body Trim Angles," *AIAA Journal*, Vol. 30, No. 4, 1992, pp. 999–1007.

[3]Park, C., and Yoon, S., "Fully Coupled Implicit Method for Thermochemical Nonequilibrium Air at Suborbital Flight Speeds," *Journal of Spacecraft and Rockets*, Vol. 28, No. 1, 1991, pp. 31–39.

[4]Griffith, B. J., and Maus, J. R., "Explanation of the Hypersonic Longitudinal Stability Problem—Lessons Learned," *Shuttle Performance: Lessons Learned*, NASA CP-2283, 1983, pp. 347–379.

Filmwise Condensation on Nonisothermal Horizontal Elliptical Tubes with Surface Tension

Sheng-An Yang*
National Kaohsiung Institute of Technology, Taiwan, Republic of China
and
Cha'o-Kuang Chen†
National Cheng-Kung University, Taiwan, Republic of China

Received Aug. 7, 1992; revision received Dec. 28, 1992; accepted for publication Dec. 29, 1992. Copyright © 1993 by the American Institute of Aeronautics and Astronautics, Inc. All rights reserved.

*Associate Professor, Department of Die-Making Engineering.
†Professor, Department of Mechanical Engineering.

Nomenclature

a, b = semimajor, semiminor axis of ellipse
C_p = specific heat of condensate at constant pressure
g = acceleration due to gravity
$h, \bar{h}$ = local, mean condensing heat transfer coefficient
k = thermal conductivity of condensate
Pr = Prandtl number
x, y = coordinate measuring length along circumference from top of tube, normal to x
μ = absolute viscosity of condensate
ρ, ρ_v = density of condensate, vapor
σ = surface tension coefficient in the film

I. Introduction

THE origin Nusselt[1] model for filmwise condensation of a quiescent vapor along an isothermal vertical plate equated gravity and viscous forces and assumed a linear temperature profile across the condensate layer. Nusselt did not consider film acceleration and energy convection effects. Afterward, many investigators, such as Rohsenow,[2] Churchill,[3] and Memory and Rose[4] have directed their effort at studying the impact of Nusselt's assumptions under such conditions and made significant improvements on Nusselt condensation theory.

Our major aim of this Note is intended to help the easy use of the Nusselt-Rohsenow-type condensation analysis with further account for the effect of surface tension by developing analytical, explicit, and straightforward integrating solutions for the problem of laminar-film condensation onto horizontal elliptical tubes, including vertical plates and horizontal circular tubes, under wall temperature variations.

II. Analysis

Consider a horizontal elliptical tube with its major axis "$2a$" oriented in the direction of gravity, situated in a quiescent pure vapor which is at its saturation temperature T_{sat}. The wall temperature T_w is nonuniform and below the saturation temperature. Thus, condensation occurs on the wall and a

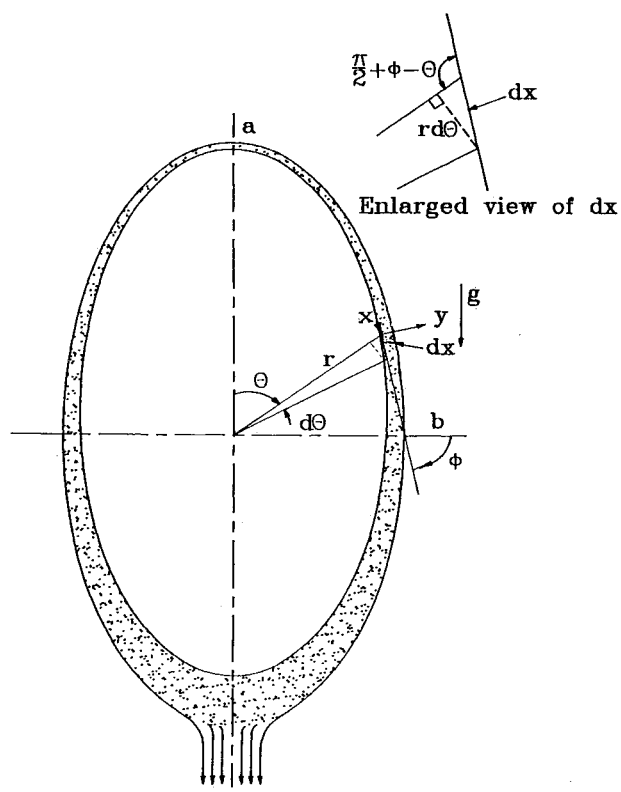

Fig. 1 Schematic and coordinate system for the condensate film flow on the elliptical surface.

continuous film of the liquid runs downward over the tube. The physical model under consideration is shown in Fig. 1.

For a laminar, steady-state condensate film with constant fluid properties, the Nusselt's local mass flow rate is expressible in terms of the local film thickness $\delta(x)$ without reference to the history of the film up to this location as

$$\dot{m} = \rho(\rho - \rho_v)\frac{g\delta^3}{3\mu}[\sin\phi + Bo(\phi)] \tag{1}$$

where $\phi = \phi(x)$ is the angle between the normal to gravity and the tangent to the tube wall at the positon (r, θ). Here, θ is the angle measured from the tube upper generatrix; r is the radial distance from the centroid of the ellipse and can be expressed as

$$r = a[(1 - e^2)/(1 - e^2\cos^2\theta)]^{0.5} \tag{2}$$

where $e = \sqrt{a^2 - b^2}/a$ is an ellipticity of the ellipse. Additionally, the pressure gradient due to surface tension forces $Bo(\phi)$ can be derived as

$$Bo(\phi) = \frac{3e^2}{2Bo}\left(\frac{1 - e^2\sin^2\phi}{1 - e^2}\right)^2 \sin(2\phi) \tag{3}$$

where $Bo = (\rho - \rho_v)ga^2/\sigma$, the Bond number.

The heat flux at the liquid-vapor interface is related to the rate of condensation by

$$h_{fg'}\frac{d\dot{m}}{dx} = k\frac{dT}{dy} = k\frac{\Delta T}{\delta} \tag{4}$$

where $h_{fg'} = h_{fg} + 0.68C_p\Delta T$, latent heat of condensation corrected for condensate subcooling by Rohsenow[2] and $\Delta T = T_{sat} - T_w$. Inserting $\dot{m}$ into Eq. (4) gives

$$\frac{\rho(\rho - \rho_v)g}{3\mu}h_{fg'}\frac{d}{dx}\{\delta^3[\sin\phi + Bo(\phi)]\} = \frac{k}{\delta}\Delta T \tag{5}$$

With reference to Fig. 1, the differential elliptical arc length may be written as

$$dx = \frac{r\,d\theta}{\cos(\phi - \theta)} \tag{6}$$

By using the geometric relationship for the tangent to the elliptical surface, one has

$$\tan\phi = \tan\theta/(1 - e^2) \tag{7}$$

In order to compare the condensate film flow hydrodynamics and heat transfer characteristics with circular tubes, based on the same condensing surface area, or same perimeter per unit length of tube, one may introduce an equivalent diameter D_e as

$$D_e = 2\frac{a}{\pi}\int_0^\pi [(1 - e^2)/\sqrt{(1 - e^2\sin^2\phi)^3}]\,d\phi \tag{8}$$

and dimensionless streamwise length s as

$$s = \int_0^\phi (1 - e^2\sin^2\phi)^{-3/2}\,d\phi \Big/ \int_0^\pi (1 - e^2\sin^2\phi)^{-3/2}\,d\phi \tag{9}$$

Once the wall temperature distribution specified or fitted by the experimental datas, one may calculate the mean wall temperature as

$$\overline{T_w} = \frac{2a}{\pi D_e}\int_0^\pi T_w(\phi)[(1 - e^2)/\sqrt{(1 - e^2\sin^2\phi)^3}]\,d\phi \tag{10}$$

and express the temperature difference across the film as

$$T_{sat} - T_w = (T_{sat} - \overline{T_w})F_t(\phi) = \overline{\Delta T}F_t(\phi) \tag{11}$$

where $F_t(\phi)$ is the nonisothermality function.

Substituting Eqs. (6) and (11) into Eq. (5), and introducing transformation of variable from x to ϕ, one obtains the local film thickness at ϕ as follows:

$$\delta^* = \delta\left[\frac{D_e k\mu\Delta T/g}{h_{fg'}\rho(\rho - \rho_v)}\right]^{-1/4} = F(\phi) \times \left\{\frac{1}{\pi}\int_0^\pi [(1 - e^2)/\sqrt{(1 - e^2\sin^2\phi)^3}]\,d\phi\right\}^{-1/4} \tag{12}$$

where

$$F(\phi) = [\sin\phi + Bo(\phi)]^{-1/3}\left\{2(1 - e^2)\int_0^\phi F_t(\phi) \times [\sin\phi + Bo(\phi)]^{1/3}(1 - e^2\sin^2\phi)^{-3/2}\,d\phi\right\}^{1/4} \tag{13}$$

It should be noted here that in the lower half of tube $(\pi/2 < \phi < \pi)$, $Bo(\phi)$ is negative and getting small with increasing ϕ in magnitude, so that the value of $\sin\phi + Bo(\phi)$ decreases from positive value to zero at the critical angle $\phi = \phi_c$. Thus, δ approaches infinity as ϕ goes up to ϕ_c. The critical angle ϕ_c is usually interpreted to mean that the liquid condensate is dripping off the tube, and less than π for $1/Bo > 0$ cases. The Nusselt-type condensation theory always assumes $\phi_c = \pi$. In fact, it is certainly conceivable that separation of the condensate layer may occur in an adverse pressure gradient environment due to retarding surface tension $[Bo(\phi) < 0]$ in the lower half of tube.

In terms of condensing heat transfer, interpreting the result of the model is straightforward by employing the usual idea of a heat transfer coefficient as follows:

$$Nu = (hD_e/k) = (Ra/Ja)^{1/4}/\delta^* \tag{14}$$

where

$$Ra = \rho(\rho - \rho_v)gPrD_e^3/\mu^2$$

$$Ja = C_p\overline{\Delta T}/h_{fg'}$$

From Eqs. (1), (4), (6), (7), and (11), the condensate production is derived as

$$\dot{m} = \frac{1}{3}\left[\frac{64k^3a^3\Delta\bar{T}^3\rho(\rho - \rho_v)g}{\mu(h_{fg'})^3}\right]^{1/4} \times \left\{(1 - e^2)\int_0^{\phi_c}\frac{F_t(\phi)[Bo(\phi) + \sin\phi]^{1/3}}{(1 - e^2\sin^2\phi)^{3/2}}\,d\phi\right\}^{3/4} \tag{15}$$

Noting that the above relation gives only half of the condensate mass flow from the tube, one finds that an energy balance within the condensate film over an entire elliptical perimeter per unit tube length yields

$$2\dot{m}h_{fg'} = \bar{h}(\pi D_e)\overline{\Delta T} \tag{16}$$

With the help of $\dot{m}$, one may obtain the overall mean Nusselt number as

$$\overline{Nu} = (\bar{h}D_e/k) = (128/81\pi)^{1/4}(Ra/Ja)^{1/4}S_f \tag{17}$$

where

$$S_f = \left\{ \int_0^{\phi_c} \frac{F_t(\phi)[\sin\phi + Bo(\phi)]^{1/3}}{(1 - e^2\sin^2\phi)^{3/2}}\, d\phi \Big/ \int_0^{\pi} (1 - e^2\sin^2\phi)^{-3/2}\, d\phi \right\}^{3/4}$$

and the mean Nusselt number up to ϕ_c as

$$\overline{Nu}_{\phi_c} = (\pi/\phi_c)(128/81\pi)^{1/4}(Ra/Ja)^{1/4}S_f \qquad (18)$$

In the limit case $e = 1$, it is noted that an elliptical tube becomes a vertical plate of both sides occurring condensation.

III. Results and Discussion

According to Lee et al.'s[5] experimental result for laminar-film condensation on a horizontal circular tube, the wall temperature distribution is approximately fitted by

$$F_t(\theta) = 1 - A\cos(\theta) \qquad (19)$$

Similarly, for general elliptical tubes, its wall temperature distribution can be approximately assumed or fitted by

$$F_t(\phi) = 1 - A\cos(\phi) \qquad (20)$$

Representative numerical results for the above case of cosine distribution of wall temperature will be illustrated and discussed. It is noted that $0 \le A \le 1$; the amplitude A depends largely on the ratio of the outside-to-inside heat-transfer coefficients.

Equations (12) and (14) have been evaluated numerically for different values of $1/Bo$, and A at any s, and the result for $e = 0.9$ is shown in Fig. 2. In the upper half of the tube, the additional effect of surface tension forces due to the decreasing surface curvature makes the condensate film thinner than the one without considering the effect of surface tension. Consequently, it leads to increasing in the heat-transfer coefficient. However, in the lower half of the tube, there exists a reverse effect of the surface tension force on the film flow due to the increasing surface curvature. Thus, the condensate film will accumulate and drop off more ahead in the lower half of the tube than that in the case of $1/Bo = 0$. Hence, for the cases $1/Bo \neq 0$, one may see that δ^* goes up to infinite value before it flows down to the bottom of the tube; Nu goes down to zero before it reaches $s = 1.0$ or $\phi = \pi$.

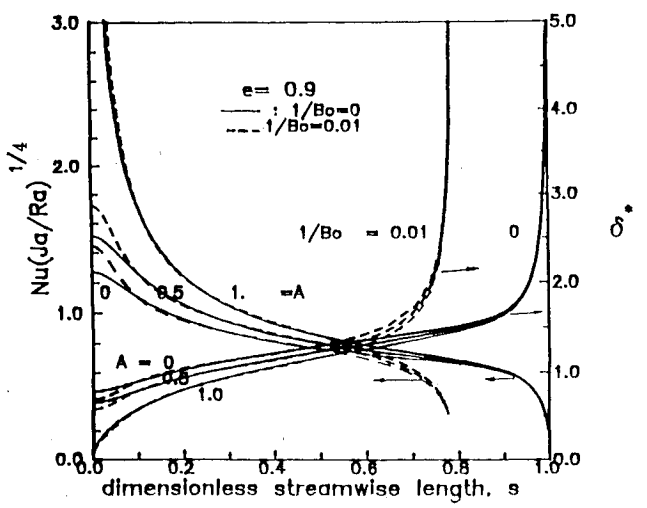

Fig. 2 Dimensionless local film thickness and heat transfer coefficient around periphery of ellipse.

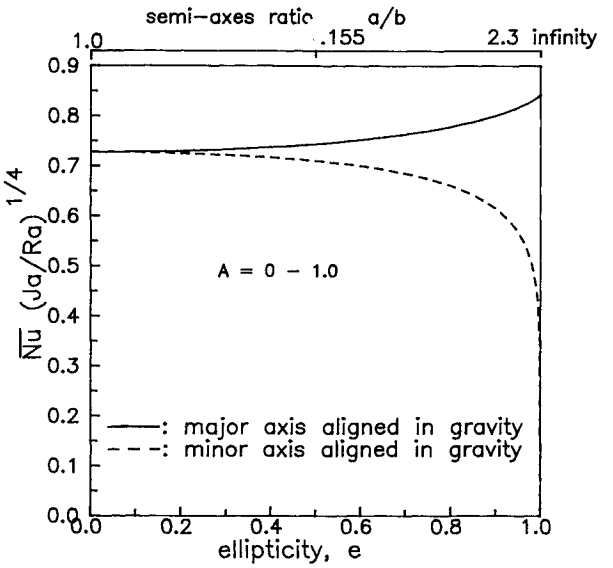

Fig. 3 Dependence of mean dimensionless heat transfer coefficient on ellipticity or semi-axes ratio.

It is also seen that the local film thickness decreases significantly with increasing A. Thus, the local heat transfer coefficient increases as A increases in the range 0–1, as shown in Fig. 2.

According to numerical results from Eq. (17), the mean heat transfer coefficient is almost unaffected by changing A as shown in Fig. 3. However, $\overline{Nu}$ increases with increasing e, very slowly at small e, and at much greater pace at large e, which agrees well with Karimi's[6] finite difference solution. For a cylinder, $e = 0$, the reduced result also coincides with Memory and Rose's[4] solution. Next, the overall mean Nusselt number is nearly unaffected by surface tension forces at small ellipticity, but is somewhat influenced at large e. For example, $e = 0.9$, its overall mean Nusselt number decreases up to 16% as the value of $1/Bo$ goes from 0 to 0.01. But from Eq. (18), the mean Nusselt number up to ϕ_c for $1/Bo \neq 0$ cases is less than that for $1/Bo = 0$ within 2%. This difference is caused by the neglected contribution due to δ going up to infinity for the region after $\phi > \phi_c$. However, the convective heat transfer coefficient due to single-phase laminar flow after ϕ_c is much less than condensing heat transfer coefficient before ϕ_c. Therefore, one may see that the above difference for $0 \le \phi \le \pi$ will actually lie between 2–16%.

IV. Concluding Remarks

Since the Nusselt (gravity drained) mode' overestimates the mean heat transfer coefficients, it should be modified by the present model using both gravity drained and surface tension drained. Although the horizontal elliptical tube with vertical major axis has higher condensing heat transfer coefficient than circular tube based on the same condensing surface area, its use may still not be justified at present due to the possible increased cost. Next, the result is quite straightforward and easily applied to a first approximation for condensation on an inclinded tube since a vertical plane passing through a circular tube yields an ellipse.

References

[1]Nusselt, W., "Die oberflachen Kondensation des Wasserdampes," *Zeitsehrift des Vereines Deutscher Ingenieure*, Vol. 60, No. 4, 1916, pp. 541–546.

[2]Rohsenow, W. M., "Heat Transfer and Temperature Distribution in Laminar Film Condensation," *Transactions of the American Society of Mechanical Engineers*, Vol. 78, No. 8, 1956, pp. 1645–1648.

[3]Churchill, S. W., "Laminar Film Condensation," *International Journal of Heat and Mass Transfer*, Vol. 29, No. 8, 1986, pp. 1219–1226.

[4]Memory, S. B., and Rose, J. W., "Free Convection Laminar Film Condensation on a Horizontal Tube with Variable Wall Temperature," *International Journal of Heat and Mass Transfer*, Vol. 34, No. 11, 1991, pp. 2775–2778.

[5]Lee, W. C., Rahbar, S., and Rose, J. W., "Film Condensation of Refrigerant 113 and Ethanediol on a Horizontal Tube—Effect of Vapor Velocity," *Journal of Heat Transfer*, Vol. 106, No. 3, 1984, pp. 524–530.

[6]Karimi, A., "Laminar Film Condensation on Helical Reflux Condensers and Related Configurations," *International Journal of Heat and Mass Transfer*, Vol. 20, No. 11, 1977, pp. 1137–1144.

Transient Thermal Mixing Following Sudden Transverse Injection of a Fluid

Fariborz Khodabakhsh,* Ramesh Konduri,†
Sastry Munukutla,‡ and Stephen Idem§
Tennessee Technological University,
Cookeville, Tennessee 38505

Introduction

THIS Note presents the results of an experiment designed to measure thermal transients induced by a sudden transverse injection of a fluid into a main flow of different temperature. Mixing problems of this nature are commonly encountered in such industrial applications as chemical processing, petroleum refining, and electrical power production. For example, in a boiling water reactor (BWR) of a nuclear power plant, reactor cleanup water is injected into the main feedwater flow. The cleanup water line is mounted transversely to the feedwater line. The temperatures of the main flow and injection flow are, in general, different from each other. A mixing region exists downstream of the injection point, wherein radial, circumferential, and longitudinal temperature gradients exist in the flow. During startup and shutdown operation, large temperature and flow rate changes occur in the mixing region. The transient fluid temperatures are strongly coupled with the pipe wall thermal response.

A search of the existing literature indicates that although a large number of references have been published on thermal mixing problems, very little work has been conducted on transient thermal mixing for transverse injection in cylindrical geometry. Pryputniewicz and Bowley[1] presented the temperature characteristics of a hot rising plume as a function of discharge Froude number and discharge depth. Salzman and Schwartz[2] investigated the trajectory and dispersion of a solid-gas jet injected into a transverse stream. Kamotani and Greber[3] and Chassaing et al.[4] examined the longitudinal and transverse distributions of velocity, temperature, and turbulence intensity of turbulent circular jets issuing into a crossflow. Wu et al.[5] studied four slotted cross section jets in crossflow and compared their behavior with circular jets. Unsteady jets were also investigated. Oosthuizen[6] studied the behavior of heated air jets discharged vertically from "shaped" circular nozzles into still air. Sherif and Pletcher[7] measured mean and fluctuating temperature fields of a heated jet discharging into cold water. Andreopoulos[8] presented mean temperature measurements and velocity-temperature fluctuations in a heated jet issuing perpendicularly into a cold stream at various velocity ratios. Andreopoulos[9] performed spectral analysis and flow visualization on a jet issuing perpendicularly into a developing crossflow. Sherif and Pletcher,[10] Andreopoulos,[11] and Andreopoulos and Rodi[12] measured turbulence characteristics of round jets in crossflow. Krausche and Fearn[13] studied the influence of injection angle of a round jet in a crossflow on vortex properties.

Amos and Moody[14] presented a procedure for predicting temperature loadings for thermal stress calculations in thick-walled pipes. It was shown that the longitudinal temperature gradient in a thick-walled pipe will cause less thermal stress than would be predicted from thin-walled theory. Konduri et al.[15] described an experiment on a one-fourth scale model designed to simulate the mixing process that occurs in the feedwater line of a BWR nuclear powerplant following transverse injection of hot reactor cleanup water. The transient temperature response of the pipe wall in the mixing region was found to vary in a first-order manner.

Experimental Program

A water flow loop was constructed in order to investigate the effects of suddenly mixing two fluid streams of different temperatures. The scale model experiment was designed to simulate the thermal mixing process which occurs in the main feedwater line of a BWR power plant. The flow rates in the main feedwater line and in the injection line were determined by means of orifice plates which had been calibrated in situ. Wall temperatures were monitored at different locations in the test section by means of copper-constantan thermocouples mounted flush with the pipe wall. For a complete description of the test setup and a discussion of experimental uncertainties, refer to Konduri et al.[15]

Two types of transient flows were studied. In the first type, water at room temperature was flowing steadily in the main feedwater line while the "hot" water was injected suddenly through the injection line. This type of test is referred to as hot injection. In the second type, the main feedwater flow was initially shut off by a valve. Hot injection water flow was pumped through the injection line, thereby inducing a steady flow rate through the test section of the main line. The transient was created by suddenly starting the main feedwater flow. This type of test is referred to as cold injection.

Thermal Model

In the mixing region, the transient pipe wall response was found to be first-order in nature, being described by a time constant τ. For a step change in fluid temperature, the pipe wall temperature varied exponentially with time t as

$$[(T - T_0)/(T_1 - T_0)] = \exp[-(t/\tau)] \tag{1}$$

In this case, T is the local pipe wall temperature. Note that a subscript 0 implies a feedwater line mixed value, whereas subscripts 1 and 2 denote initial feedwater and injection line values, respectively. The dimensionless time constant is defined by

$$\tau^* = [(V \cdot \tau)/X][(T_0 - T_1)/(T_2 - T_1)] \tag{2}$$

where V is the mean fluid velocity, and X is the axial distance from the injection point. The transient mixing in the mixing region depends on the turbulence level at that point. Because this is a transverse injection problem, the turbulence level depends on both the main feedwater flow and injection water flow velocities. The Reynolds number ratio Re^* is defined as the ratio of the Reynolds numbers of the main flow to that of the injection flow

$$Re^* = \frac{\rho_1 V_1 D_1/\mu_1}{\rho_2 V_2 D_2/\mu_2} \tag{3}$$

Received June 19, 1992; presented as Paper 92-2926 at the AIAA 27th Thermophysics Conference, Nashville, TN, July 6–8, 1992; revision received Dec. 15, 1992; accepted for publication Dec. 15, 1992.
Copyright © 1993 by the American Institute of Aeronautics and Astronautics, Inc. All rights reserved.

*Research Engineer, Center for Electric Power. Member AIAA.
†Research Assistant, Center for Electric Power.
‡Professor, Mechanical Engineering. Associate Fellow AIAA.
§Assistant Professor, Mechanical Engineering. Member AIAA.